

2



# Lawrence Berkeley Laboratory

UNIVERSITY OF CALIFORNIA

RECEIVED  
LAWRENCE  
BERKELEY LABORATORY

FEB 1 1984

LIBRARY AND  
DOCUMENTS SECTION

## Materials & Molecular Research Division

Presented in part at the Hollywood, Florida Meeting  
of the Electrochemical Society, October 5-10, 1980

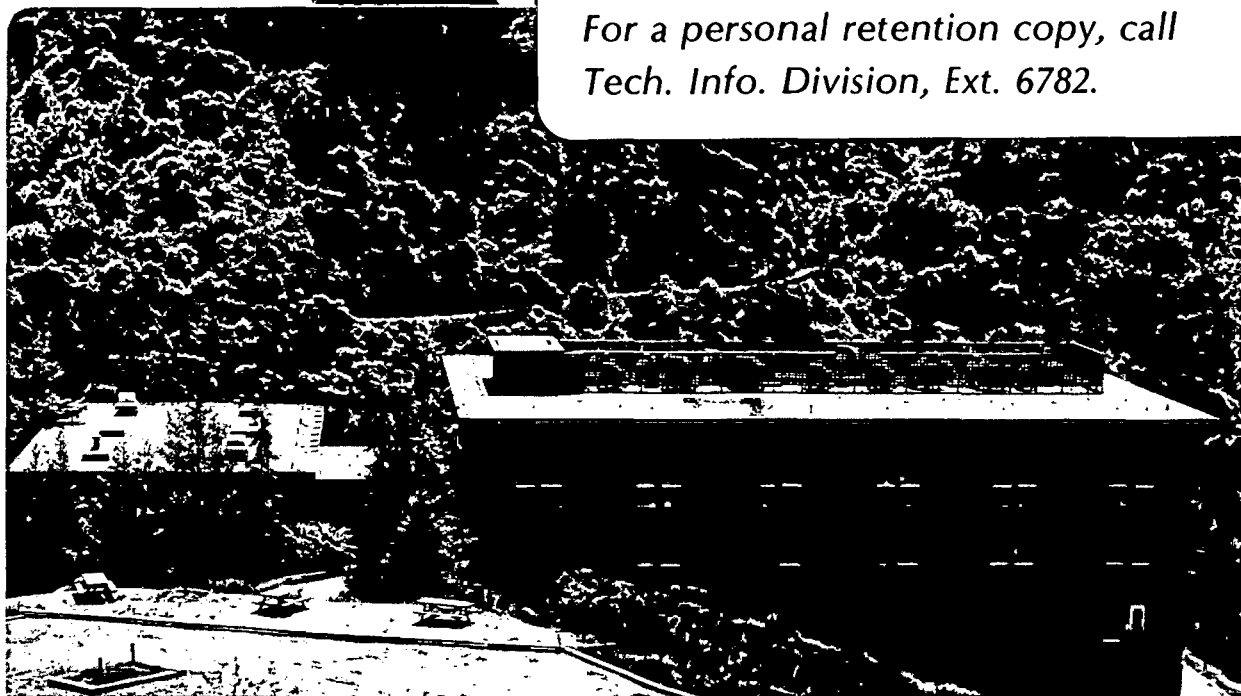
ELLIPSOMETER STUDIES OF SURFACE LAYERS ON LITHIUM

F. Schwager, Y. Geronov, and R.H. Muller

November 1981

### TWO-WEEK LOAN COPY

*This is a Library Circulating Copy  
which may be borrowed for two weeks.  
For a personal retention copy, call  
Tech. Info. Division, Ext. 6782.*



LBL-13657  
2

## DISCLAIMER

This document was prepared as an account of work sponsored by the United States Government. While this document is believed to contain correct information, neither the United States Government nor any agency thereof, nor the Regents of the University of California, nor any of their employees, makes any warranty, express or implied, or assumes any legal responsibility for the accuracy, completeness, or usefulness of any information, apparatus, product, or process disclosed, or represents that its use would not infringe privately owned rights. Reference herein to any specific commercial product, process, or service by its trade name, trademark, manufacturer, or otherwise, does not necessarily constitute or imply its endorsement, recommendation, or favoring by the United States Government or any agency thereof, or the Regents of the University of California. The views and opinions of authors expressed herein do not necessarily state or reflect those of the United States Government or any agency thereof or the Regents of the University of California.

ELLIPSOMETER STUDIES  
OF SURFACE LAYERS ON LITHIUM

F. Schwager,<sup>\*</sup> Y. Geronov<sup>†</sup> and R. H. Muller

Materials and Molecular Research Division  
Lawrence Berkeley Laboratory  
University of California  
Berkeley, CA 94720

ABSTRACT

The growth of surface layers on lithium in propylene carbonate solutions can be followed by ellipsometry, although the refractive indices of many potential film materials are close to those of the electrolyte. Film thicknesses calculated from ellipsometer measurements increase over periods of several days at open circuit; they are several times larger than those derived from galvanostatic pulse measurements. Films are found to be inhomogeneous with properties continuously varying as a function of distance from the substrate; compact regions are located adjacent to the metal and porous regions adjacent to the solution. Electrode capacitance measurements are sensitive to the thin compact region which can also be generated by reaction with water vapor. Ellipsometer measurements are primarily affected by the thicker, porous region which may be formed by the precipitation of decomposition products of the solution.

---

<sup>\*</sup> Present address: Mettler Instruments AG, CH-8606 Greifensee, SWITZERLAND.

<sup>†</sup> Permanent address: Central Laboratory of Electrochemical Power Sources, Bulgarian Academy of Sciences, Sofia, BULGARIA

## INTRODUCTION

Surface layers formed under open circuit conditions on lithium in propylene carbonate (PC) solvent and its solutions of lithium perchlorate and lithium hexafluoroarsenate have been investigated by ellipsometry. The present study was conducted in conjunction with galvanostatic pulse measurements reported earlier,<sup>1</sup> and the results obtained by the two techniques are compared.

## EXPERIMENTAL

Ellipsometric and electrochemical measurements were conducted in situ in a hermetically sealed polypropylene cell consisting of an electrode compartment with two strain-free quartz windows arranged for 75° angle of incidence of the light beam, and a solution container located above the electrode compartment. (Fig. 1) This configuration enables one to take measurements very soon after the electrode is brought in contact with the solution. The ellipsometer used was of the self-compensating type in the Polarizer - Quarter wave plate - Sample - Analyzer - configuration.<sup>2</sup> Corrections for component imperfections were derived from four-zone measurements. A mercury lamp (150 W with interference filter for the wavelength of 5461 Å) and an argon-ion laser (Lexel Model 75 at a wavelength of 5145 Å) were used as light sources. The mercury lamp could be used only for smooth, well reflecting electrode surfaces.

Working and counter electrodes consisted of high purity (Foote) lithium disks, of 25mm diameter and 3mm thickness. The cross-section of a freshly extruded lithium wire of 1mm diameter served as reference electrode. The working electrodes were prepared by scraping the lithium with a scalpel and pressing it with a polycarbonate sheet in a recirculating purified helium atmosphere (<0.5 ppm O<sub>2</sub>, H<sub>2</sub>O, 5 ppm N<sub>2</sub>) as described

previously.<sup>1</sup> No significant difference between the native film of an electrode which was only cleaned and one which was also pressed was found by depth profiling Auger Spectroscopy (PHI model 590). Solutions of  $\text{LiClO}_4$  or  $\text{LiAsF}_6$  with and without added water were investigated, their preparation has also been described before.<sup>1</sup> In the purified helium atmosphere the electrodes were inserted in the electrode compartment and the solution compartment was filled with electrolyte. The closed cell was then transferred to air for conducting the measurements. A delay of about one minute after contact of the electrodes with solution was required to optically align the cell.

Film growth was followed simultaneously by ellipsometry and electrochemical pulse techniques. After the experiment, the working electrode was washed with pure propylene carbonate, dried and transferred into an UHV-chamber for Auger spectroscopy and ellipsometry of the dry film.

### RESULTS

The ellipsometric results are presented as plots of the relative amplitude change  $\psi$  vs. the relative phase change  $\Delta$  due to reflection. Figure 2 shows a plot obtained for film growth on lithium in propylene carbonate of low water content (~10 ppm) without salt and with 1 M  $\text{LiClO}_4$ . The immersion time is indicated on both curves. The presence of the electrolyte has a great effect on the rate of film formation. Ellipsometer parameters  $\psi$  and  $\Delta$  change faster for lithium immersed in pure PC, indicating faster film growth. However, both electrochemical measurements at the end of the experiment (small amounts of salt were added to provide conductivity) as well as depth profiling with Auger spectroscopy

indicate the presence of a thin film, which shows a nonporous appearance in micrographs. Scanning electron micrographs have shown that film formation (by corrosion or precipitation) on lithium in PC with small amounts of added water is faster than in PC -  $\text{LiClO}_4$  solutions with the same amount of added water.<sup>1</sup> The difference between electrochemical and ellipsometric measurement for pure PC with no water added is, at present, difficult to explain. It may involve the formation of a poorly adhering, highly porous film and its loss during the rinsing and drying operations.

Ellipsometer measurements of film growth in solutions of 0.5M and 1.0M  $\text{LiClO}_4$  in PC did not show much difference. Addition of water to  $\text{LiClO}_4$  - solutions seems to slow down the rate of film formation slightly (Fig. 3). This finding is in agreement with electrochemical measurements<sup>1</sup> where it was also found that films formed in these solutions are less conductive.

$\text{LiAsF}_6$  - solutions form much thicker films in a shorter time than  $\text{LiClO}_4$  - solutions (Fig. 4). This result emphasizes the importance of the anion for film formation and is in agreement with the findings from electrochemical measurements.

Elemental film compositions were determined by Auger spectroscopy. Typical spectra are given in Fig. 5. The prominent peaks are those for carbon and oxygen. Films grown in  $\text{LiClO}_4$  solution show a small chlorine content. No arsenic could be detected in films grown in  $\text{LiAsF}_6$  solution. Depth profiles given in Fig. 6 indicate composition continuously varying with depth. A positive secondary ion mass spectrum (SIMS) given in Fig. 7 shows a large number of peaks between mass 2 and 50.

To investigate the precipitation of solution decomposition products as a possible mechanism for the formation of porous layers, a polished silver surface was used as an inert electrode in 1M  $\text{LiClO}_4$  in PC. Ellipsometer measurements on this surface showed only small changes which could be interpreted as the growth of a highly porous layer. SEM micrographs of the same surface showed discrete hillocks, which were principally composed of C, O and Cl, according to the Auger spectrum. Positive ion SIMS showed 3 principal mass peaks above 60, namely 63 ( $\text{H}_3\text{CO}_3^+$ , not present in the film, Fig. 7), 73 and 81.

## DISCUSSION

### Optical Models

Two features in the  $\Delta/\psi$ - plots of Figs. 2-4 are characteristic: the first one is a loop at the beginning of the experiment, the second an almost straight section with ever-increasing  $\psi$ - values at the later stages of the experiment. Calculations have shown that the real part of the refractive index of the film is primarily responsible for the size of the loop, the imaginary part for the slope of the straight part. (Fig. 8). Refractive indices for some possible film materials, solution and substrate are listed in Table I. It was not possible to fit the experimental results satisfactorily with calculated values assuming a homogeneous film with refractive indices for any of the materials listed or their combination with solution in a uniformly porous film. Film thicknesses indicated along the theoretical curves of Fig. 8 are also much larger than those

derived by capacitance measurements, which reach values of 200-400 $\overset{\circ}{\text{A}}$  at the most. This discrepancy indicates a more complex film structure. Micrographs of a film grown in a 1M LiClO<sub>4</sub>/PC- solution for 2 weeks indeed show densely packed particles of approximately 2000-3000 $\overset{\circ}{\text{A}}$  diameter.

In an attempt to reconcile the results obtained by electrochemical transient techniques and those obtained by ellipsometry, a dual film model was investigated (Fig. 9 inset). In this model, both films are assumed to be homogeneous. The bottom film (Film 2) is a thin (max. 200-400 $\overset{\circ}{\text{A}}$ ) nonporous dielectric which is responsible for the electrode capacitance. The upper film (Film 1) is thick and porous and is mainly responsible for the ellipsometer measurement.

The dual film model provides a means to explain the discrepancy between ellipsometric and electrochemical results and gives improved, although not satisfactory, agreement between experimental and theoretical  $\Delta/\psi$ - plots. It was found that a rather high real part of the refractive index of the bottom films had to be assumed. Literature values for different lithium compounds (Table I) show that LiCl or Li<sub>2</sub>O would have to be present in a mixture with low refractive index compounds to account for values of 1.55 and higher. Li<sub>2</sub>CO<sub>3</sub> which had been proposed as the film material<sup>3, 4, 5</sup> shows too low a refractive index to be the primary constituent of the bottom (barrier) film. Polymerization products of the solvent, which had also been suggested as film material<sup>6,7</sup> could make up the top film. Depth profiling by Auger spectroscopy showed that only small amounts (~2 At %) of chlorine (for which Auger spectroscopy is very sensitive) but large amounts of oxygen (35-50 At %) are present in the film. Lithium oxide is thermodynamically the favored product of a reaction

between Li and water, (or oxygen) which could be present in sufficient amounts in the solution. Keil, et al.<sup>8</sup> found in gas phase experiments, that oxygen reacts faster than water with Li. Auger peaks at 37 and 31 eV found in films are attributed<sup>8</sup> to Li in  $\text{Li}_2\text{O}$ . A dual-film structure of adsorbed oxygen and porous lithium carbonate has been proposed by Leif and Gilmour.<sup>9</sup>

In order to improve agreement with ellipsometer measurements in the first stages of film growth, several inhomogeneous film models with continuously varying refractive index (Fig. 10) were investigated. Real and imaginary part of the complex refractive index was assumed to decrease from the metal/film boundary to the film/solution boundary. Such an inhomogeneity could be due to variable porosity. It was found that predictions based on a linear profile of refractive index were in best agreement with the experimental results. Again, a rather high value of the real part of the refractive index had to be chosen for the part of the film close to the substrate; at the film/solution interface the refractive index of the film was chosen to be equal to that of the solution.

Figure 11 illustrates the satisfactory agreement between experimental results and calculations based on a linear profile of the refractive index. The loop in the curve is determined by the high real part at the bottom of the film. The small imaginary part is introduced to adjust the slope of the curve at the later stages of growth and indicates a slightly absorbing film. Light absorption in the film could be due to nonstoichiometry or the presence of F- centers. F- centers have been extensively studied for lithium halides. According to Hunderi,<sup>10</sup> the F- center excitation energy for LiOH should be about the same as that for LiCl.

The model of a porous inhomogeneous film with continuously variable refractive index (or porosity) has been tested in a different way. By changing the refractive index of the immersion medium from a value of 1.43 for the solution to 1.0 for vacuum, one can change the effective refractive index of a film with fluid-filled pores drastically as illustrated for a homogeneous porosity in Fig. 12. A realistic physical film model should produce the same film thickness for measurements in solution and in vacuum, if the pore structure remains the same in the two immersion media. Table II shows a comparison of film thicknesses obtained from ellipsometer measurements in solution and in vacuum for a linear and a parabolic profile of the film refractive index with the same values at the inner and outer edge. The data support a refractive index (or porosity) varying linearly with thickness.

#### Film Growth

Film growth derived from ellipsometer and galvanostatic pulse measurement are presented in Fig. 13. An approximately parabolic rate law (exponent 1.6) holds for film growth derived from capacitance measurements, (curve a, Fig. 14, based on a dielectric constant  $\epsilon = 4.9$  corresponding to  $\text{Li}_2\text{CO}_3$ ). Film growth derived from ellipsometer measurements (curve b, Fig. 14) follows a near-linear rate law initially (exponent 0.7) but seems to approach the parabolic law later (exponent 1.5). A parabolic rate law (exponent 2.2) has also been found to hold for film growth with water vapor (Fig. 14, curve c). Figure 15 shows ellipsometer measurements and interpretation for the latter case.

## CONCLUSIONS

Ellipsometer measurements have shown that surface layers on lithium are inhomogeneous with porosity increasing approximately linearly from a dense region facing the electrode to a highly porous region facing the liquid. The refractive index of the dense region is higher than that of  $\text{Li}_2\text{CO}_3$  or  $\text{LiOH}$  and supports the presence of  $\text{Li}_2\text{O}$ . Ellipsometer measurements qualitatively agree with results obtained by electrochemical transient techniques (except for film growth in pure PC), because the dense region only is detected by electrical measurements.

Films are formed more rapidly in pure propylene carbonate than in the presence of electrolyte salts.  $\text{LiClO}_4$  solutions form slower growing (more protective) films than  $\text{LiAsF}_6$  solutions. Perchlorate also reduces the effect of water. Reaction with water is the most likely origin of the dense region and its protective properties are confirmed by the parabolic rate law. A continuing growth of the porous region, could indicate a different film origin and precipitation of insoluble products resulting from the decomposition of the solution may be a contributing factor.

## ACKNOWLEDGMENT

This work was supported by the Assistant Secretary for Conservation and Renewable Energy, Office of Advanced Conservation Technologies, Electrochemical Research Division of the U.S. Department of Energy under contract No. DE-AC03-76SF00098. We thank Mr. Kenneth A. Gaugler for taking the Auger and SIMS spectra and Mr. Walter T. Giba for design and construction of the cell.

This paper was presented, in part, at the Hollywood, Florida Meeting of the Electrochemical Society, Oct. 5-10, 1980 Extended Abstract #37.

REFERENCES

1. Y. Geronov, F. Schwager and R. H. Muller, J. Electrochem. Soc., 129, 1422 (1982).
2. H. J. Mathieu, D. E. McClure and R. H. Muller, Rev. Sci. Instrum. 45, 798 (1974).
3. F. P. Dousek, J. Jansta and J. Riha, J. Electroanal. Chem., 46, 281 (1973).
4. A. N. Dey, Thin Solid Films, 43, 131 (1977).
5. A. N. Dey in "Lithium Nonaqueous Battery Electrochemistry," E. B. Yeager, B. Schumm, Jr., G. Blomgren, D. R. Blankenship, V. Leger and J. Akridge, eds., Electrochem. Soc., Pennington, NJ, 1980, p 83.
6. M. Garreau and J. Thevenin, J. Microsc. Spectrosc. Electron. 3, 27 (1978).
7. I. Epelboin, M. Froment, M. Garreau, J. Thevenin and D. Warin in "Power Sources for Biomedical Implantable Applications and Ambient Temperature Lithium Batteries," B. B. Owens and N. Margalit, eds., Electrochem. Soc., Princeton, NJ, 1980, p. 417.
8. R. Keil, J. Hoenigman, W. Modeman, T. Wittenberg and J. Peters, AFWAL-TR-80-2018, Interim Tech. Report, Univ. Dayton Res. Inst., 10/79.
9. G. A. Leif and A. Gilmour, J. Appl. Electrochem. 9, 663 (1979).
10. O. Hunderi, Surf. Sci. 57, 451 (1976).

Table I. Refractive index of potential film materials, solution and substrate 5461 Å wavelength.

---

LiOH	1.466
Li <sub>2</sub> CO <sub>3</sub>	1.50
Li <sub>2</sub> O	1.644
LiCl	1.662
PC, 1M LiClO <sub>4</sub>	1.429
Li	0.25 - 2.3i

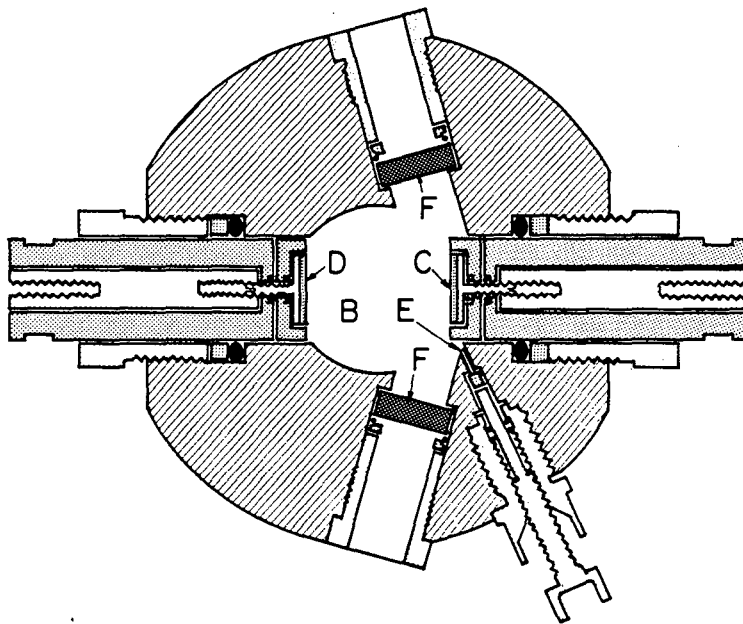
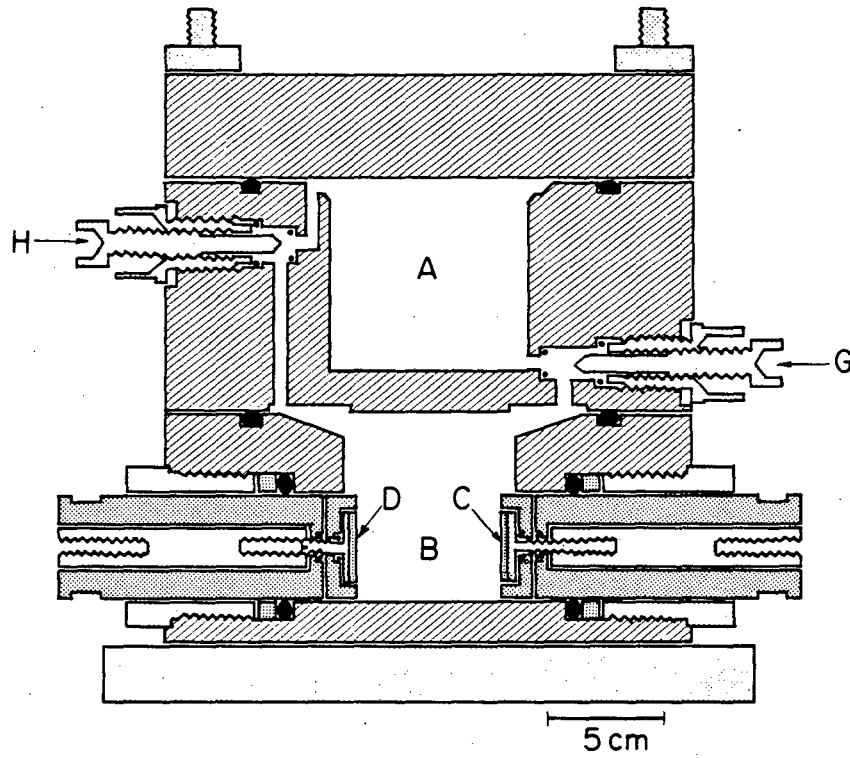
Table II. Film thickness derived from ellipsometer measurements in solution and in vacuum for linear and parabolic refractive index profiles. Refractive index at bottom of film  $1.57-0.02i$ , at top  $1.4293$  in solution,  $1.0$  in vacuum.  $1 \text{ M LiClO}_4$  in PC,  $1000 \text{ ppm H}_2\text{O}$  added.

Refractive index Profile	Thickness	
	solution	vacuum
linear	$1500 \text{ \AA}$	$1550 \text{ \AA}$
parabolic	$1950 \text{ \AA}$	$2350 \text{ \AA}$

FIGURE CAPTIONS

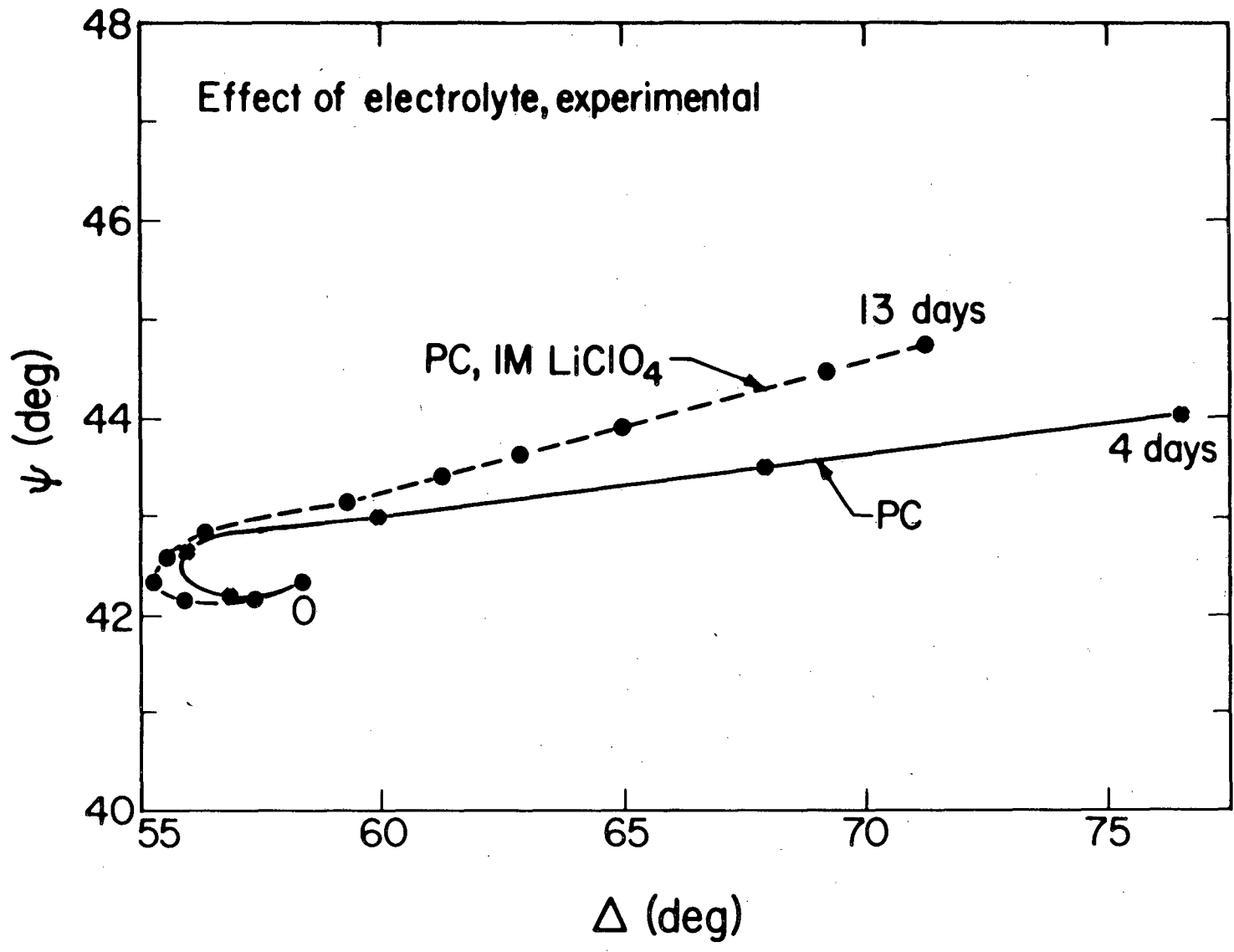
- Fig. 1. Non-aqueous cell for ellipsometry and potential measurements on lithium electrodes immediately after contact with electrolyte, vertical and horizontal cross-sections. A - reservoir, B - cell, C - working electrode, D - counter electrode, E - reference electrode, F - windows, G - liquid valve, H - gas valve.
- Fig. 2. Effect of the presence of electrolyte on film formation on lithium in propylene carbonate (PC). Measured ellipsometer parameters  $\psi$  and  $\Delta$ . Pure solvent (PC) and 1 M  $\text{LiClO}_4$  in PC. Period of immersion in days given along the curves.
- Fig. 3. Effect of water content of 1 M  $\text{LiClO}_4$  solution in PC on film formation. No water added (10 ppm), 0.1% water added. Measured ellipsometer parameters.
- Fig. 4. Effect of the nature of electrolyte on film formation. I - 1 M  $\text{LiClO}_4$ , II - 0.5 M  $\text{LiAsF}_6$  in PC, measured ellipsometer parameters. Period of immersion in days given along the curves.
- Fig. 5. Auger spectra of films formed after (a) 10 days in solutions of 1 M  $\text{LiClO}_4$  and (b) 7 days in 0.5 M  $\text{LiAsF}_6$ . Spectra taken after 30 sec ion etching at 2keV.
- Fig. 6. Depth profile of film formed during 9 days in 1 M  $\text{LiClO}_4$  + 500 ppm  $\text{H}_2\text{O}$ . Ion etching with 3 keV, 15 nA argon beam (approx.  $400\text{\AA}/\text{min}$ .).
- Fig. 7. Positive ion SIMS spectrum of film formed during 10 days in 1 M  $\text{LiClO}_4$ , 1 kV argon ion beam, 17nA, 14 min.
- Fig. 8. Effect of real and imaginary parts of the film refractive index on ellipsometer parameters computed for homogeneous films. Film thickness in  $\text{\AA}$  given along computed curves.

- Fig. 9. Dual film model. Computed ellipsometer parameters for a dual film (broken curve) with compact, thin bottom layer (2) and a porous, growing top layer (1). Computation for growing single film shown by solid curve. Film thickness in  $\text{\AA}$  given along curves. Dual film model shown in inset.
- Fig. 10. Models of film porosity (or refractive index) profiles (a) homogeneous, (b) inhomogeneous with linear profile, (c) inhomogeneous with parabolic profile.
- Fig. 11. Interpretation of ellipsometer measurements on Li in 1 M  $\text{LiClO}_4$  in PC with an inhomogeneous film of linear refractive index profile. Thickness of inhomogeneous film in  $\text{\AA}$  given along computed curve. Period of immersion in days given with measured points.
- Fig. 12. Effect of immersion medium on the effective refractive index of a porous film illustrated with a homogeneous film of 50% porosity, pores evacuated or filled with electrolyte.
- Fig. 13. Film growth on Li in 1 M  $\text{LiClO}_4$  in PC derived from ellipsometer measurements for a linear refractive index profile, and film growth derived from galvanostatic pulse measurements ( $\epsilon = 4.9$ ).
- Fig. 14. Rate laws for film formation on Li.  
(a) Ellipsometer measurements, 1 M  $\text{LiClO}_4$  in PC  
(b) Capacitance measurements, 1 M  $\text{LiClO}_4$  in PC,  $\epsilon = 4.9$   
(c) Ellipsometer measurements, water vapor 1 ppm in He, thickness based on  $n = 1.46$  (LiOH)
- Fig. 15. Ellipsometer parameters for film growth on Li in He with 1 ppm water vapor • - measurements 1 - 8 days, x - computation for homogeneous film,  $n = 14664$ , 0 - 1400  $\text{\AA}$ .



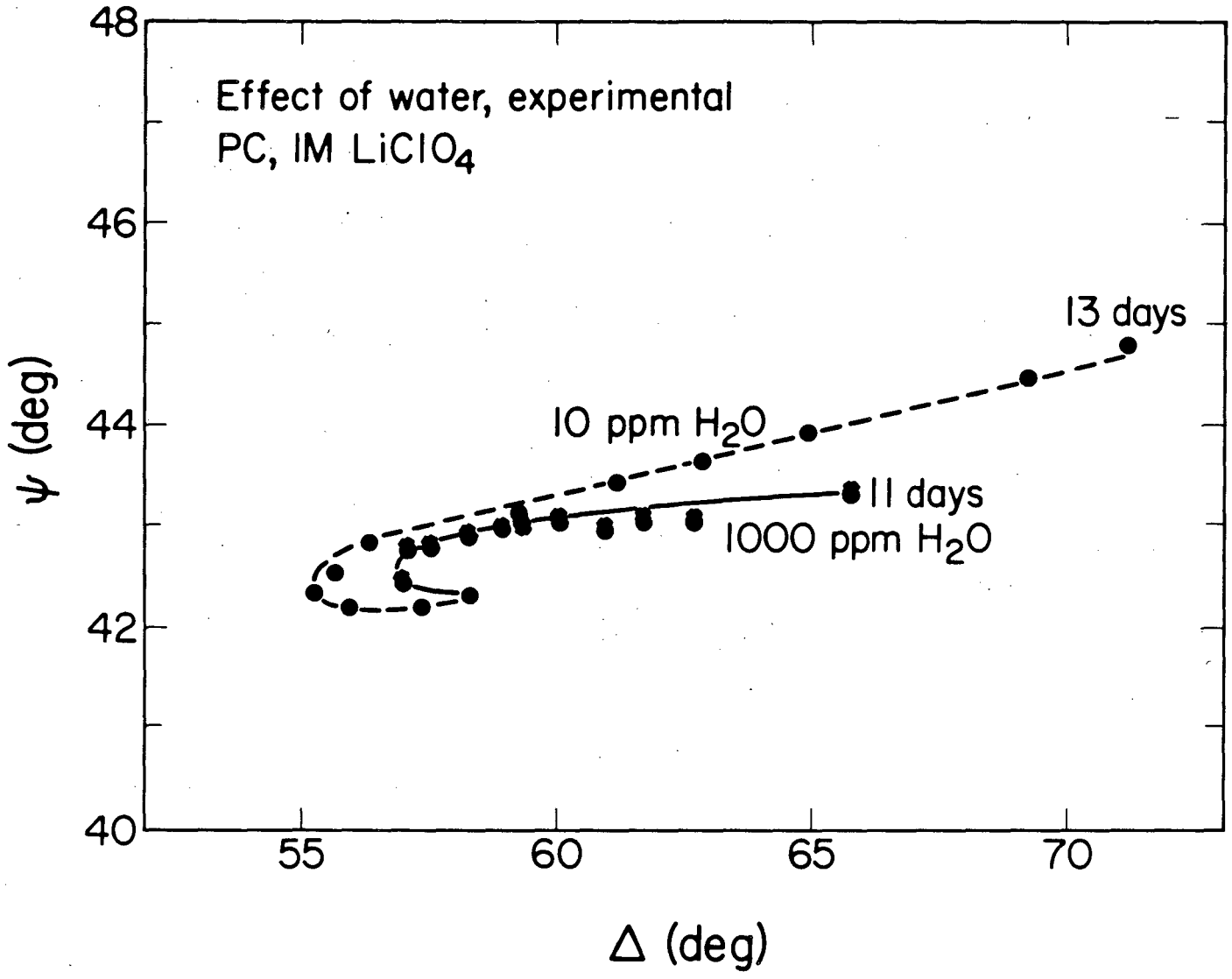
XBL8310-4031

Fig. 1



XBL 809-2042

Fig. 2



XBL 809-2044

Fig. 3

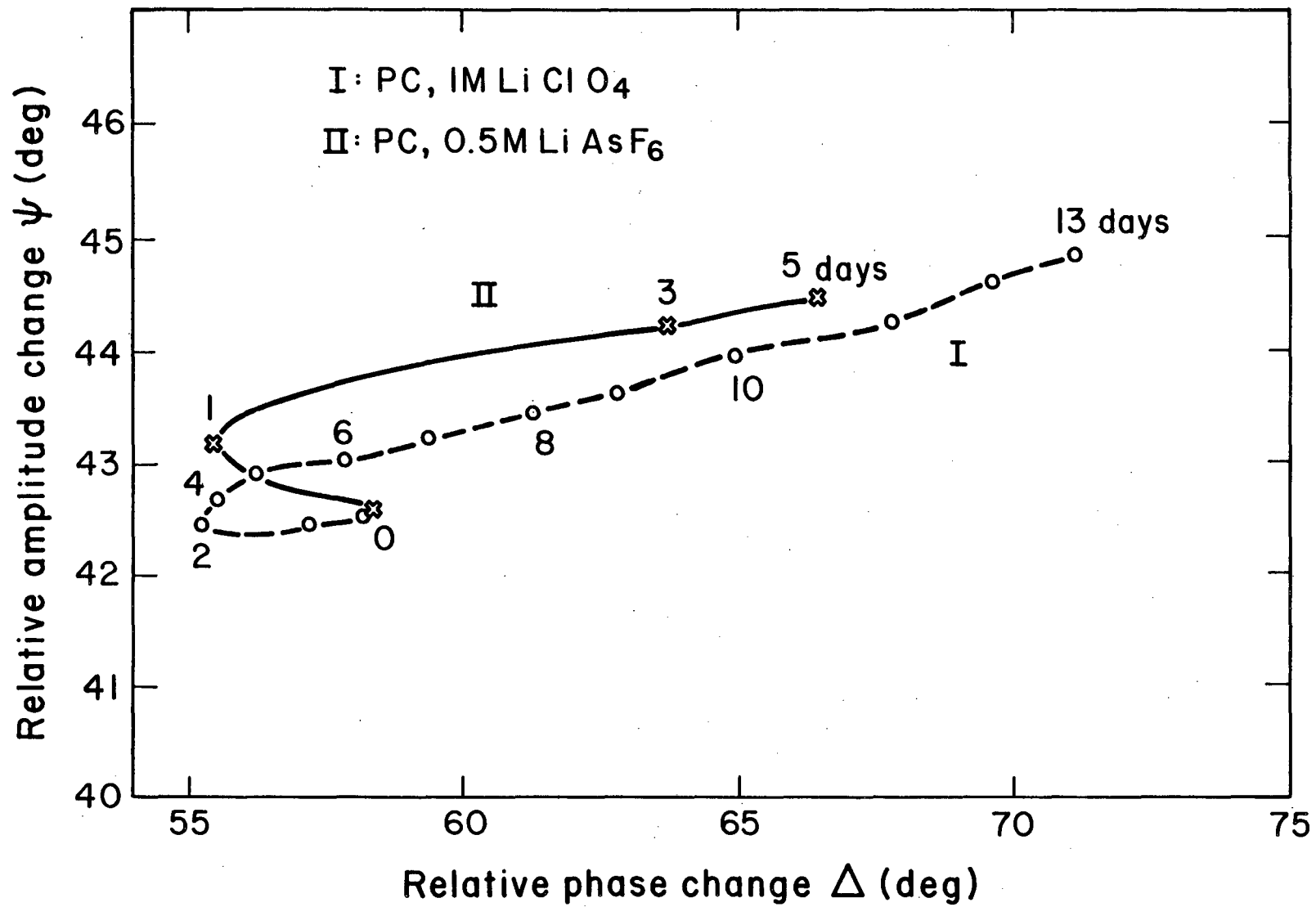


Fig. 4

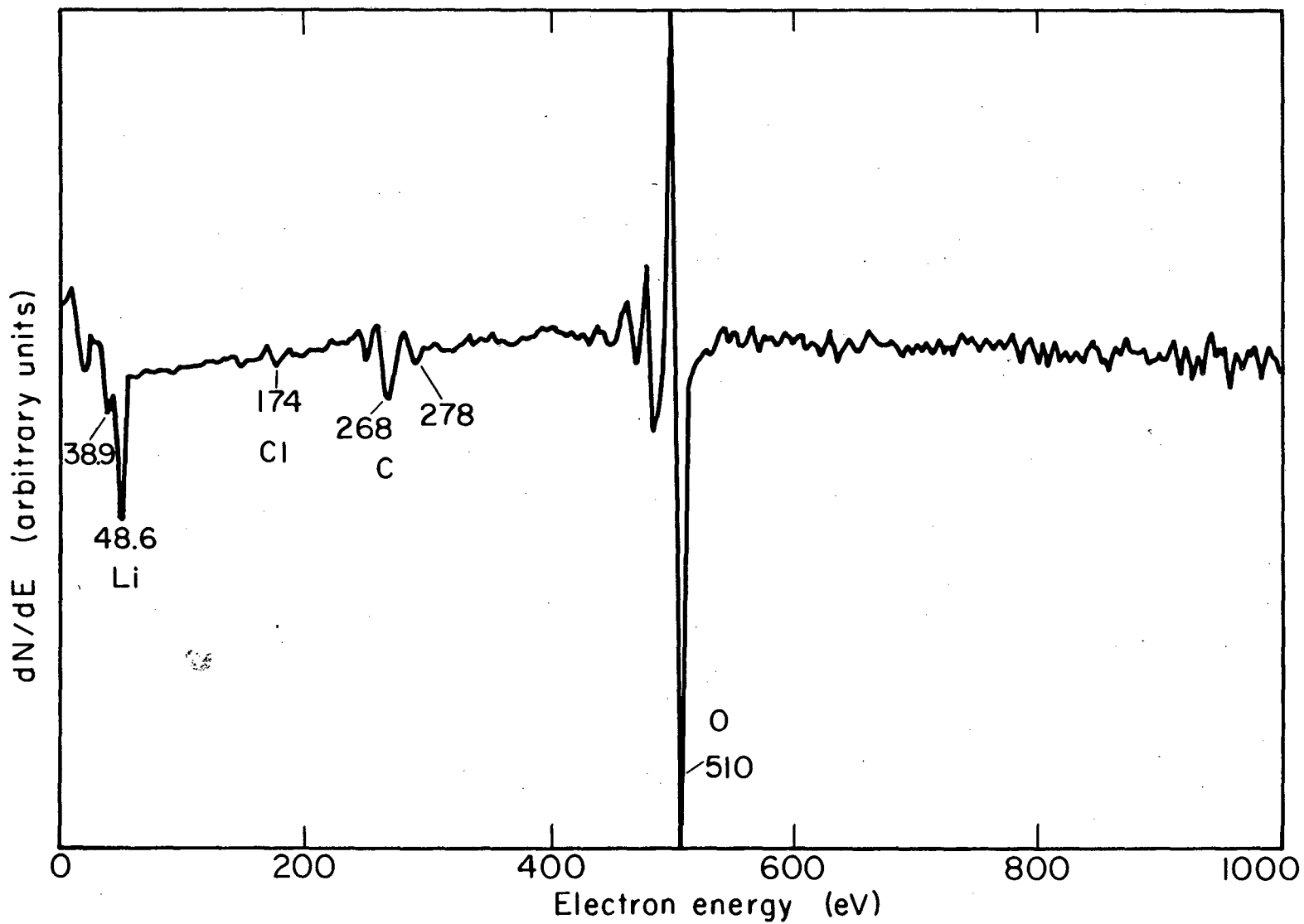
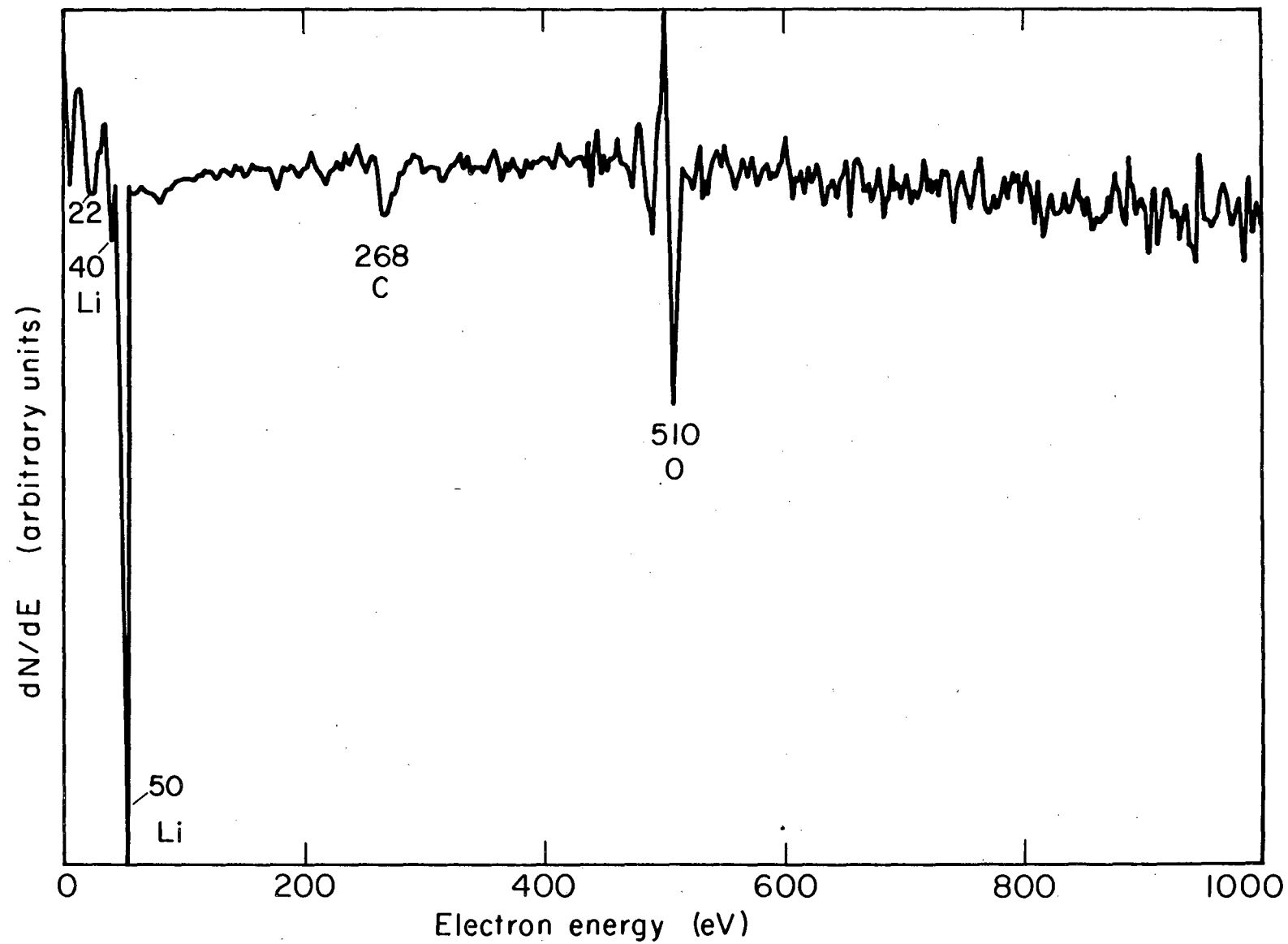


Fig. 5(a)

XBL8310-4028



XBL8310-4027

Fig. 5(b)

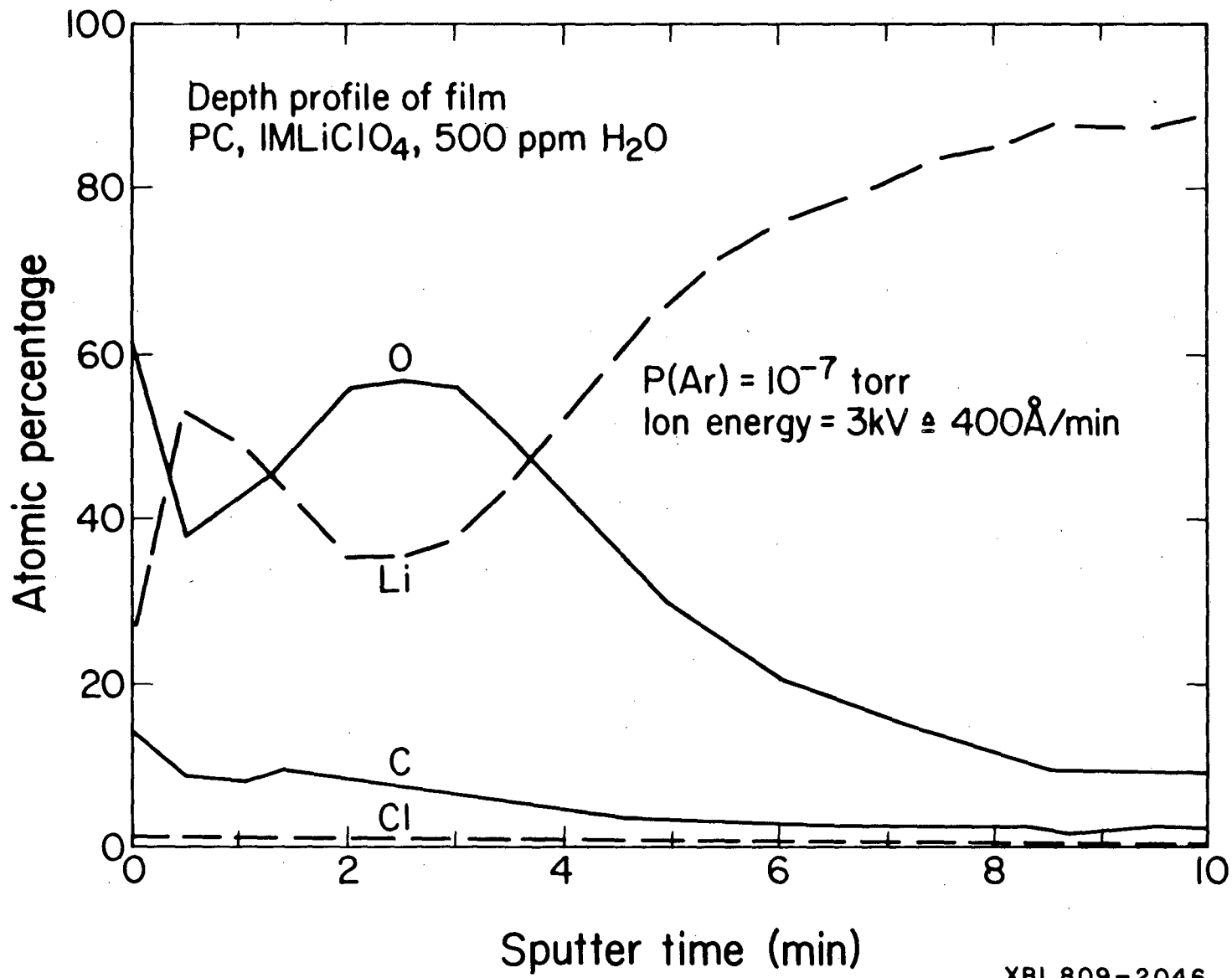
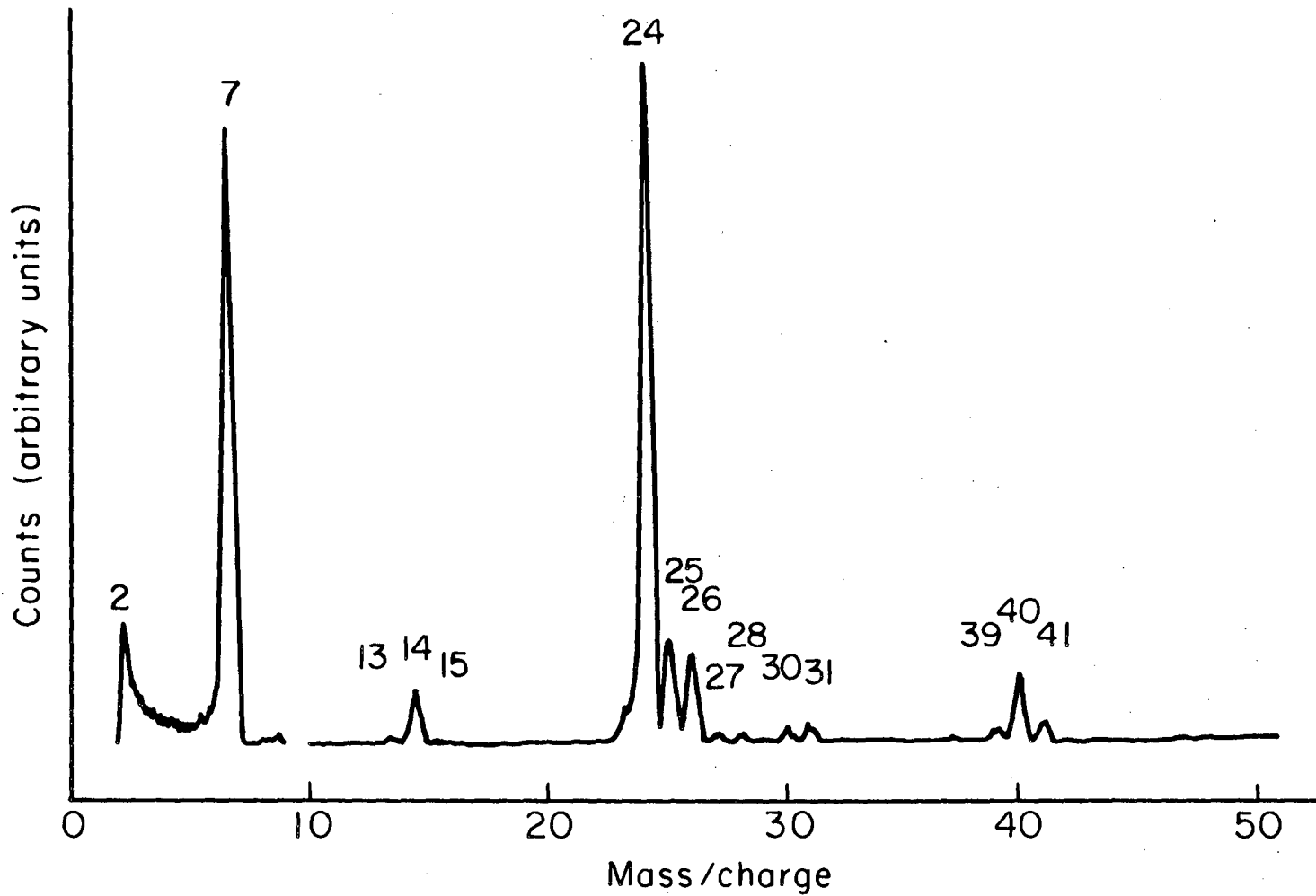


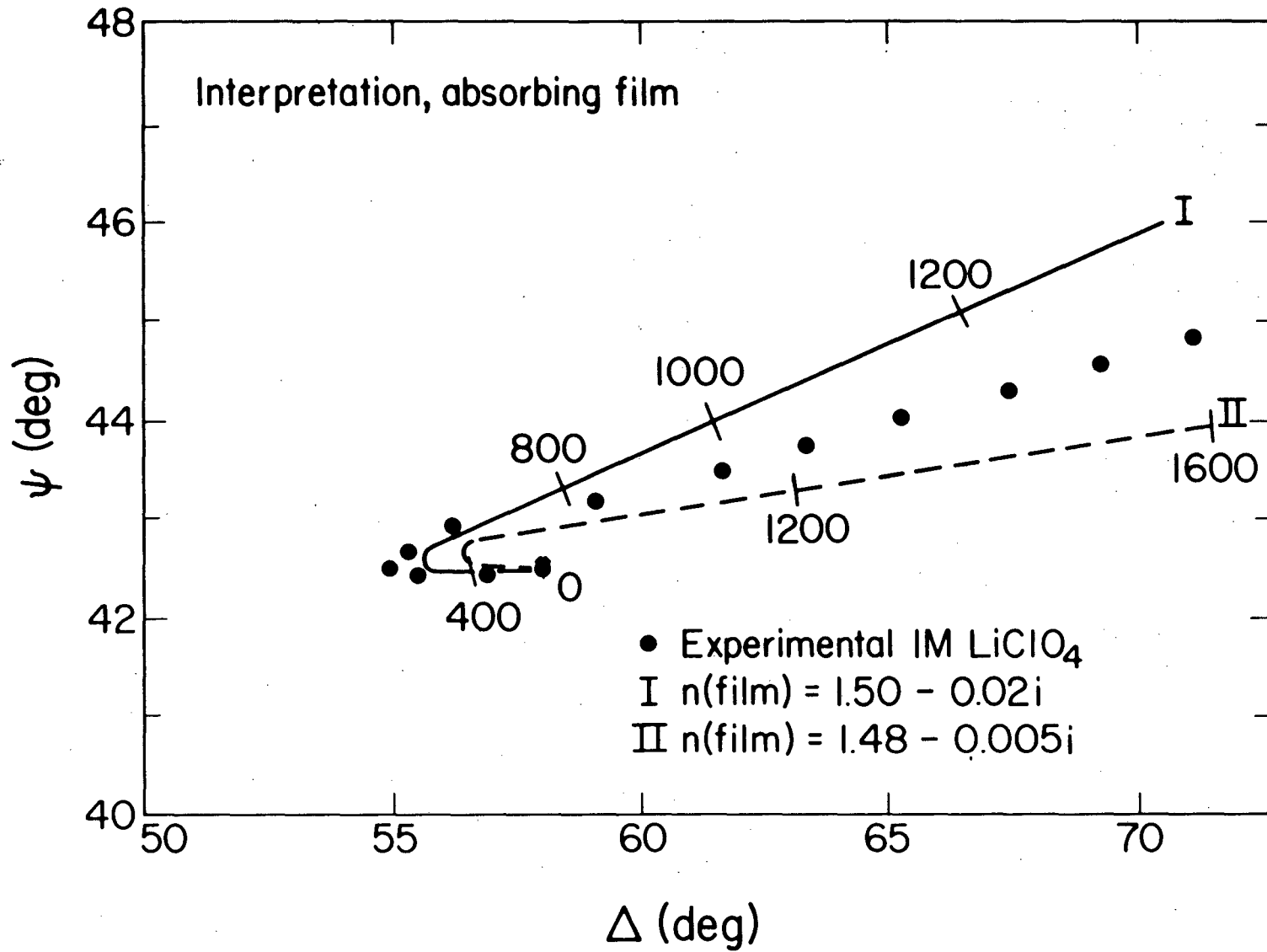
Fig. 6

XBL 809-2046



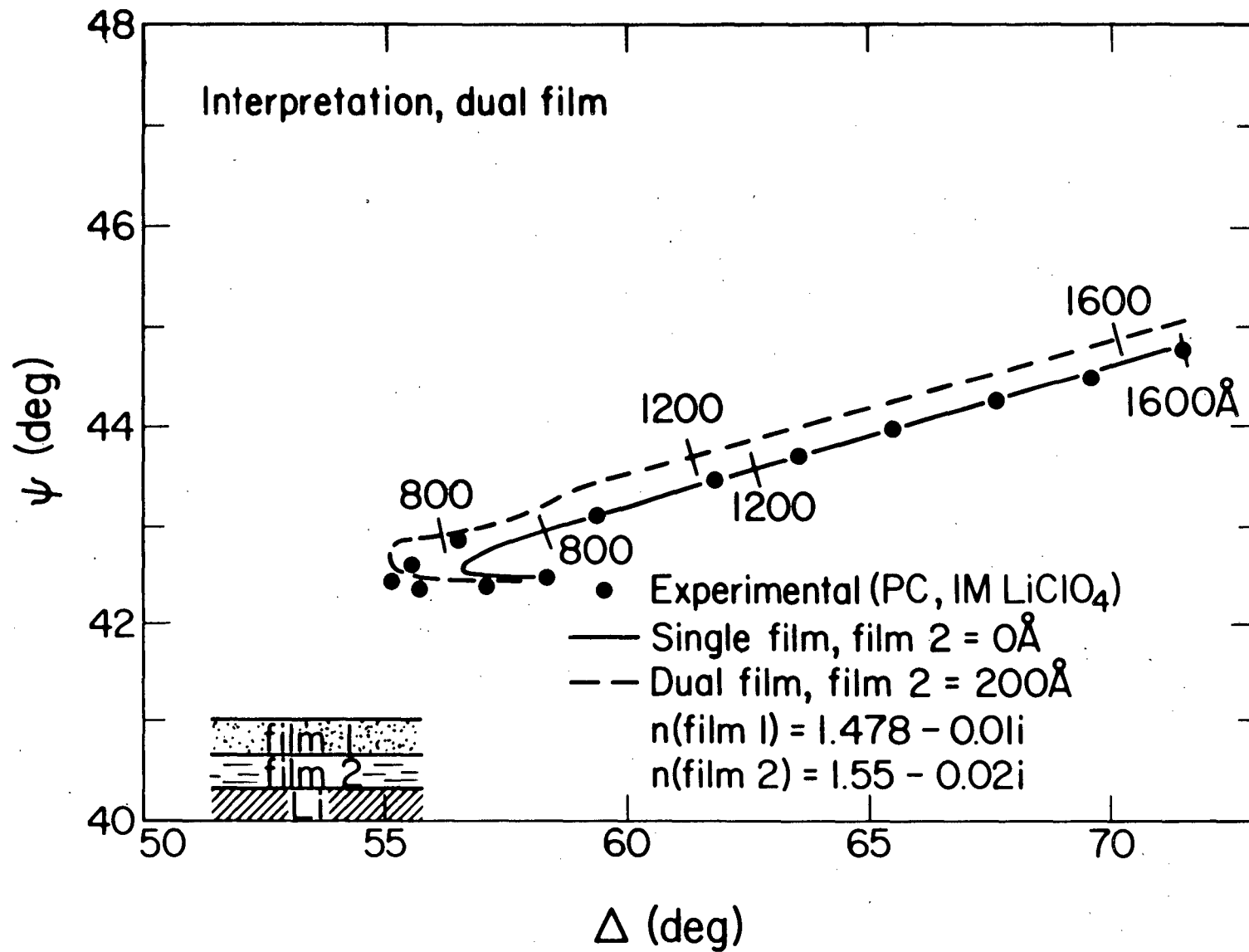
XBL8310-4026

Fig. 7



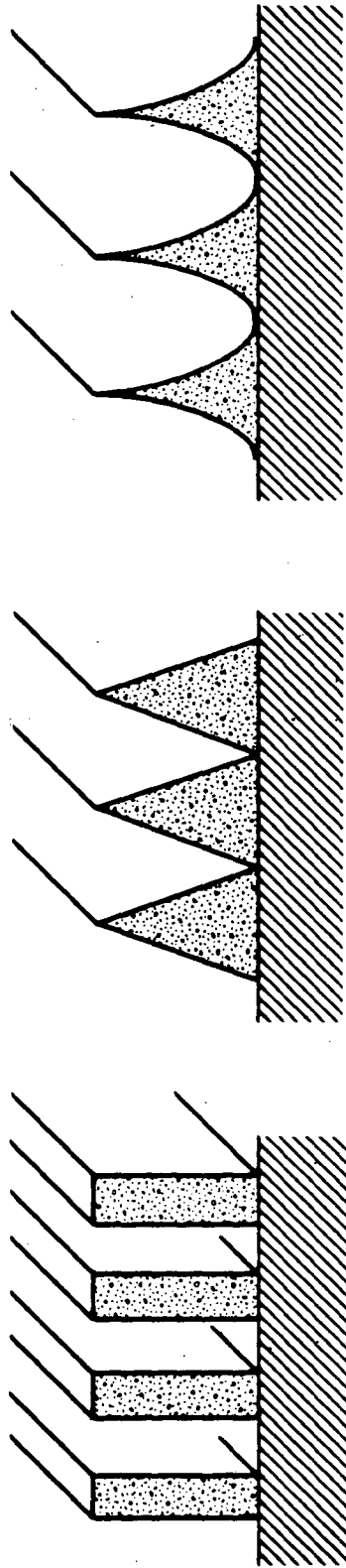
XBL 809-2048

Fig. 8



XBL 809-2041

Fig. 9



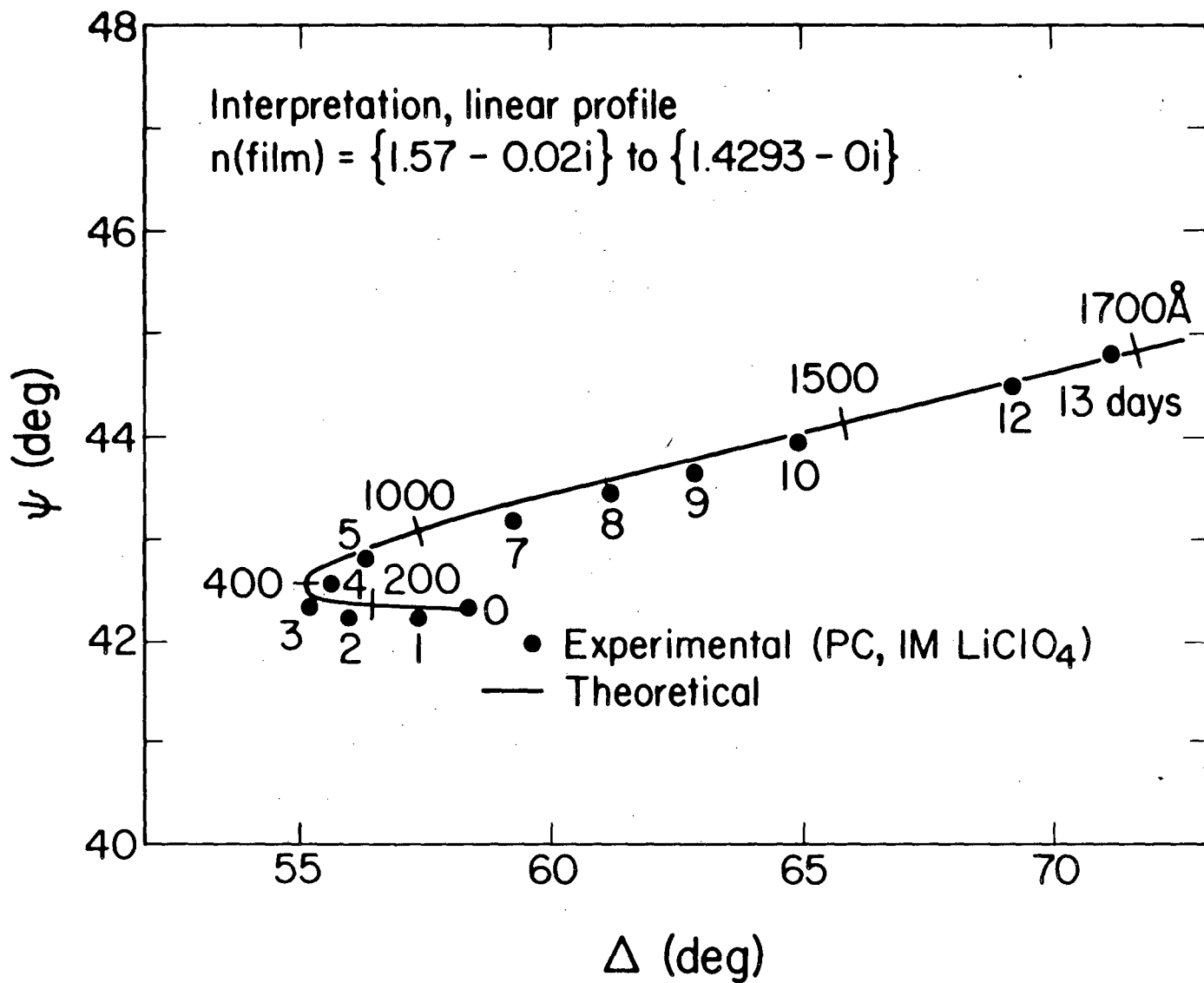
(a)

(b)

(c)

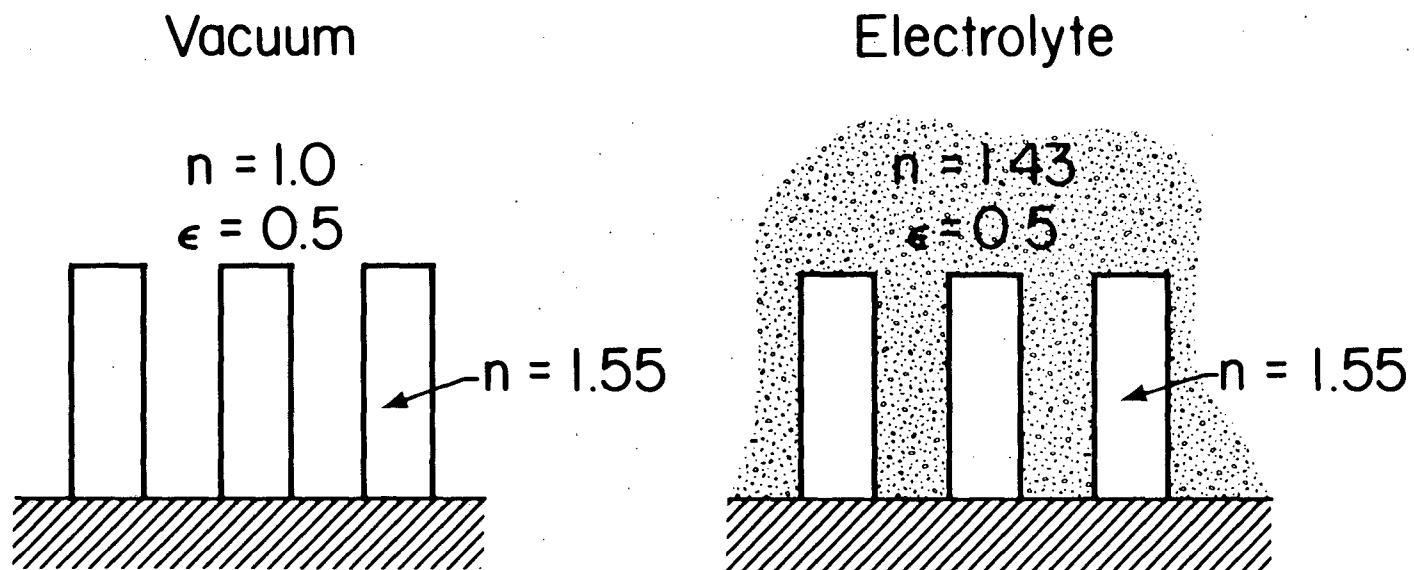
XBL 809 - 2050

Fig. 10



XBL 809-2047

Fig. 11

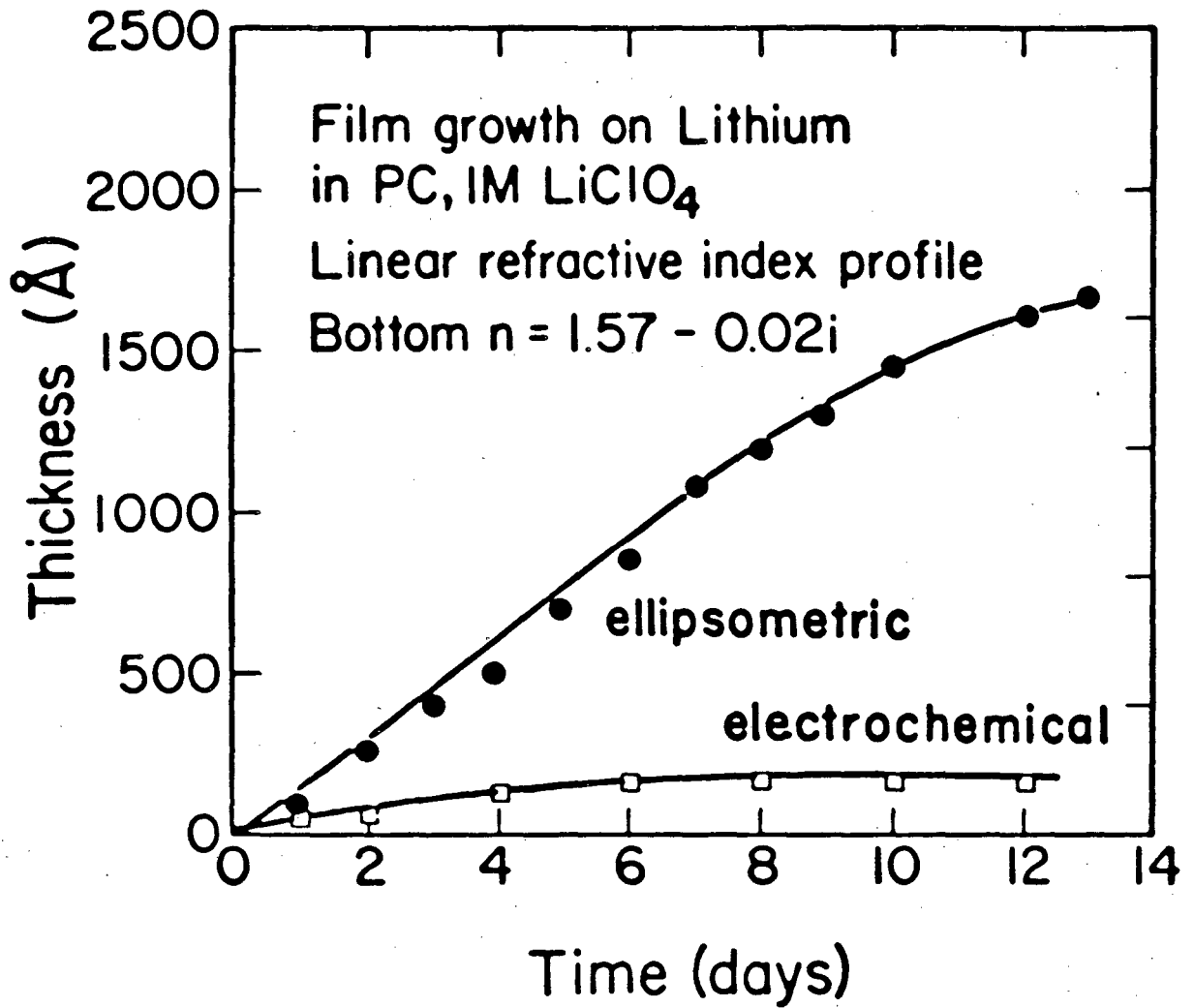


Effective  
optical constants  
of film = 1.275

1.49

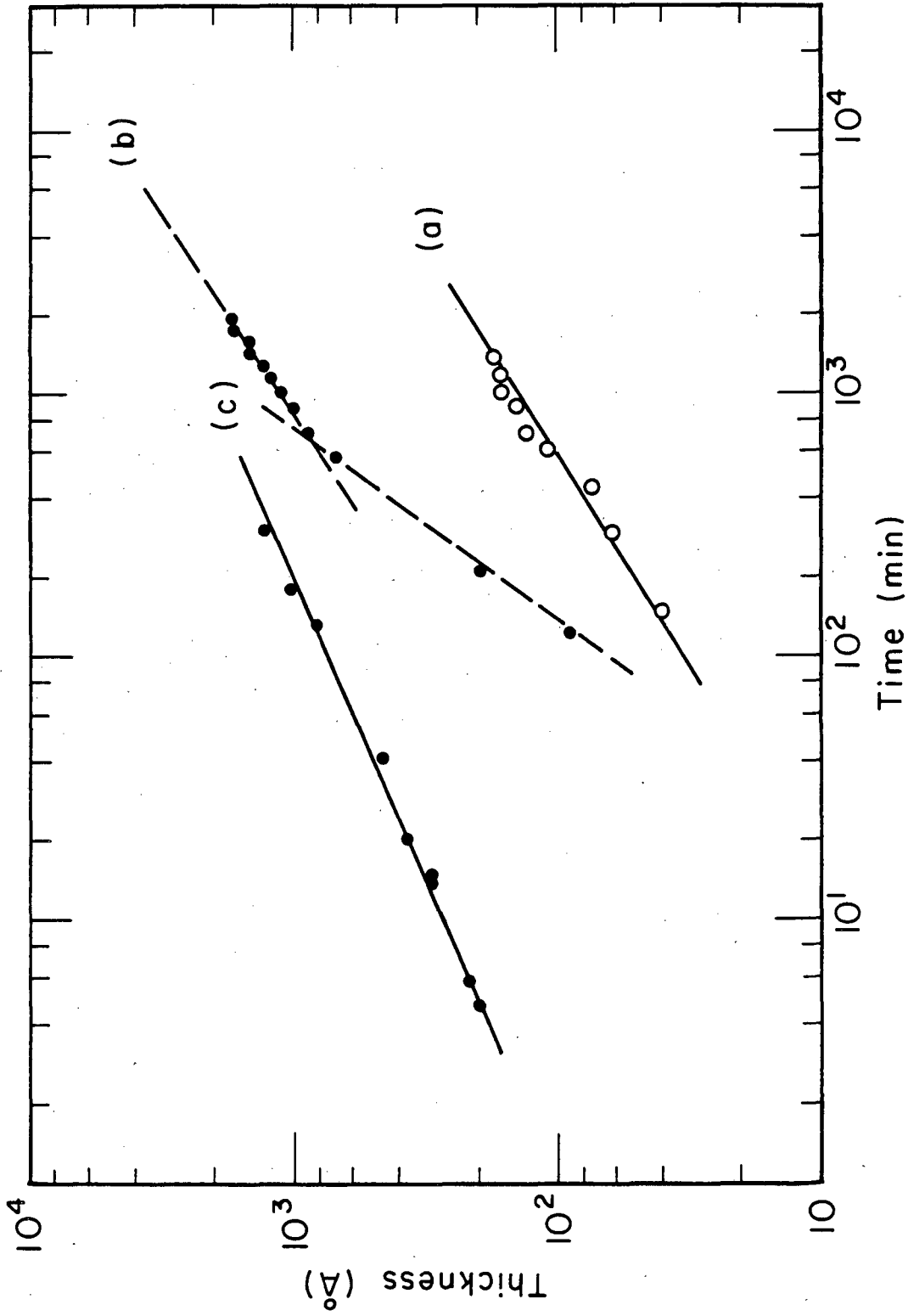
XBL 809 - 2051

Fig. 12



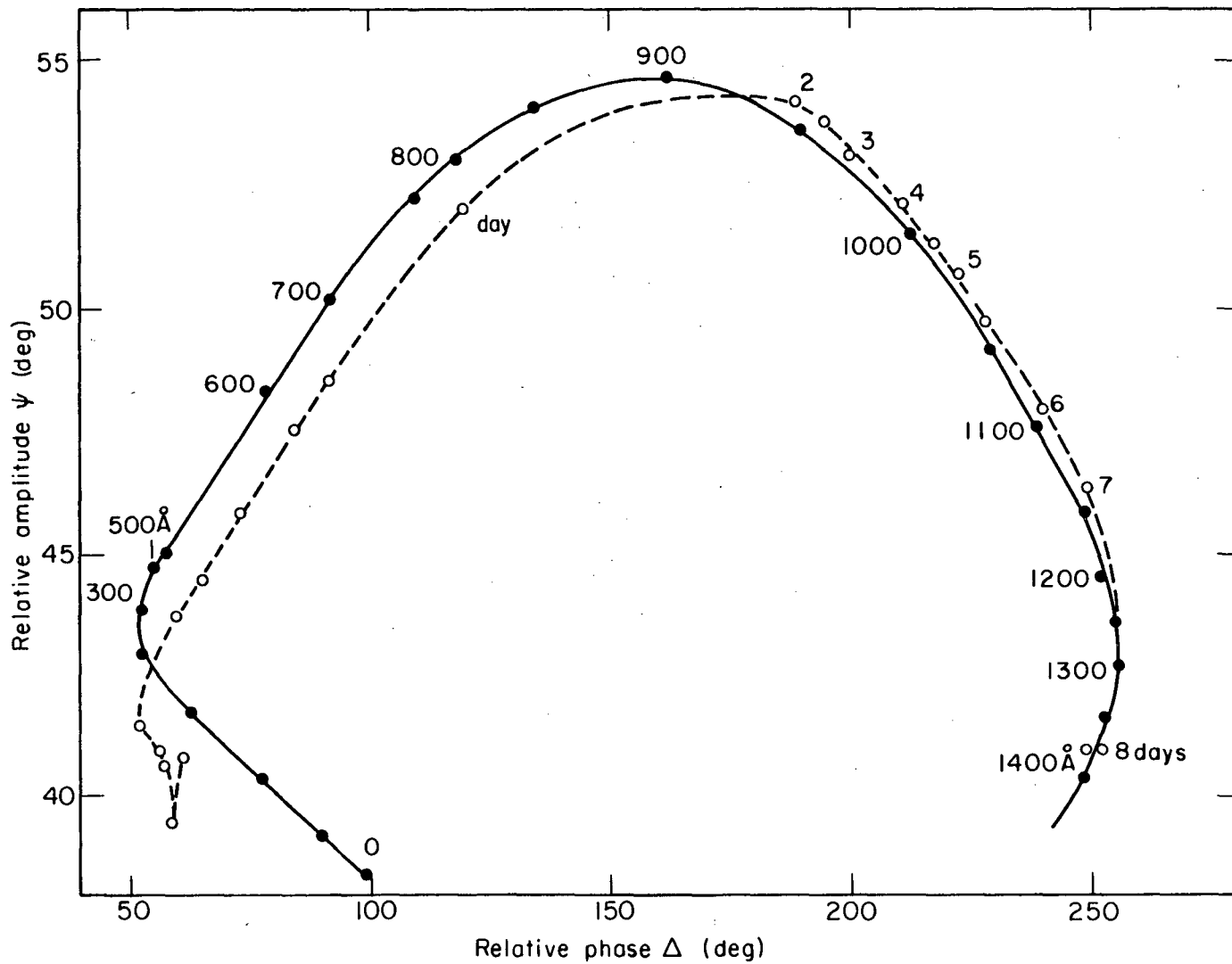
XBL 809-2043A

Fig. 13



XBL8310-4029

Fig. 14



XBL8310-4030

Fig. 15

This report was done with support from the Department of Energy. Any conclusions or opinions expressed in this report represent solely those of the author(s) and not necessarily those of The Regents of the University of California, the Lawrence Berkeley Laboratory or the Department of Energy.

Reference to a company or product name does not imply approval or recommendation of the product by the University of California or the U.S. Department of Energy to the exclusion of others that may be suitable.

TECHNICAL INFORMATION DEPARTMENT  
LAWRENCE BERKELEY LABORATORY  
UNIVERSITY OF CALIFORNIA  
BERKELEY, CALIFORNIA 94720